Multidimensional modelling of biofilm structure

C. Picioreanu[1, 2], M.C.M. van Loosdrecht[1], and J.J. Heijnen[1]

[1] Department of Biochemical Engineering, Delft University of Technology, Julianalaan 67, 2628 BC Delft, The Netherlands
[2] Department of Chemical Engineering, University Politehnica of Bucharest, Splaiul Independentei 313, 77206 Bucharest, Romania

ABSTRACT

A fully quantitative two- and three-dimensional approach for biofilm growth and structure formation has been developed. The present model incorporates the flow over the irregular biofilm surface, convective and diffusive mass transfer of substrate, bacterial growth, biomass spreading and biofilm detachment due to biofilm deformation stress. Any arbitrary shape of the carrier surface can be accommodated in the model, as well as multispecies and multisubstrate biofilms. Results of model simulations show that the ratio between nutrient transfer rate to the biofilm and the bacterial growth rate influences to a great extent the biofilm roughness and porosity. A low mass transfer rate, i.e., low Reynolds numbers or high values of Thiele modulus, results in the development of a rough and open biofilm. When the biofilm growth is limited not by substrate availability, but by the rate of bacterial metabolism, the biofilm forms as a compact and homogeneous structure. High shear forces lead, by means of continuous erosion and discrete sloughing events, to a smoother, more compact and thinner biofilm. The multidimensional biofilm modelling approach used is well suited for theoretical investigations of factors that affect biofilm structure and ecology.

Introduction

Research done over the past years has shown show that biofilms develop in a multitude of patterns [4, 6]. Traditionally, development of biofilms was seen as the formation of a layered structure growing from the substratum up. This led to the now traditional, one-dimensional biofilm models [i.e., 13] where all property gradients (e.g., substrate concentration, biomass density, porosity, etc.) vary only in the direction from the bulk liquid to the carrier surface. There is however significant spatial variability in biofilm density, porosity, surface shape, microbial activity and distribution in clusters [1, 4, 14]. Bishop and Rittmann [2] suggested that while one-dimensional models can be adequate for description alone, multidimensional modelling may be required for prediction of biofilm heterogeneity. In a model that should predict biofilm structural properties such as surface shape, porosity, pore and channel sizes, these same properties must not only be the output of the model, but they are also the boundary conditions which continuously change in time.

Modelling the structural development of a biofilm is a great challenge because of the complex interaction between many processes. The biofilm development is determined by "positive" processes like cell attachment, cell division, and polymer production, which lead to biofilm volume expansion, and "negative" processes, like cell detachment and cell death,

Microbial Biosystems: New Frontiers
Proceedings of the 8th International Symposium on Microbial Ecology
Bell CR, Brylinsky M, Johnson-Green P (eds)
Atlantic Canada Society for Microbial Ecology, Halifax, Canada, 1999.

which contribute to biofilm shrinking. By changing the balance between these processes, biofilms with different structural properties like porosity, density or surface roughness can be formed as was hypothesised by van Loosdrecht *et al.* [12] and experimentally shown by Kwok *et al.* [7].

The main biofilm expansion is due to bacterial growth and extracellular polymer production. The nutrients necessary for bacterial growth are dissolved in the liquid flow. To reach the cells they pass first through a boundary layer (external mass transfer) and then through the biofilm matrix (internal mass transfer). The external mass transfer resistance is given by the thickness of the concentration boundary layer (CBL), which is directly correlated to the hydrodynamic boundary layer (HBL) resulting from the flow pattern over the biofilm surface. We can therefore say that on one hand the fluid flow drives the biofilm growth by regulating the concentration of substrates and products at the liquid-solid interface. On the other hand, the flow shears the biofilm surface, eroding the protuberances. While the flow changes the biofilm surface, the interaction is reciprocal because a new biofilm shape leads to a different boundary condition and, thus, different flow and concentration fields. This leads further to the concept of temporal heterogeneity: the biofilm is a dynamic structure evolving in nonsteady-state conditions. However, as seen later, due to the very different magnitude of process time constants, for practical computational reasons it can be assumed that some processes are at equilibrium while others are in a dynamic or frozen regime.

For a model capable of full description of the three-dimensional heterogeneity of a biofilm, it is important that the model can easily cope with large variations in time constants and continuously changing boundary conditions. With this in mind, we started to develop a model based on a discrete algorithm (a cellular automaton approach [8, 9, 10]). Similar approaches have also been reported by Wimpenny and Colasanti [15] and Hermanowicz [5]. Despite the fact that their models generate biofilms with qualitative features resembling real biofilms, they work in a completely abstract time and space. Consequently, their model parameters are not directly correlated to the physical values of widely accepted parameters such as diffusivities or reaction rate constants. Moreover, we soon found that for some processes a traditional differential approach is more advantageous [9, 10]. This led to a combined discrete-differential model for the formation of biofilms. The general structure of this model is described below together with a few model applications.

Model Equations and Solution Algorithms

The equations describing the biofilm system in nonsteady-state are:

- total mass conservation for the fluid phase (the continuity equation):

$$\nabla \cdot \mathbf{u} = 0 \qquad \textbf{(1)}$$

- momentum conservation for the fluid flow over the biofilm (the Navier-Stokes equations):

$$\frac{\partial \mathbf{u}}{\partial t} + \mathbf{u} \cdot \nabla \mathbf{u} = -\frac{1}{\rho}\nabla p + \nu \nabla^2 \mathbf{u} \qquad \textbf{(2)}$$

- mass conservation for one dissolved component (for the limiting substrate only):

$$\frac{\partial C_S}{\partial t} + \mathbf{u} \cdot \nabla C_S = -R_S(C_S, C_X) + D\nabla^2 C_S \qquad \textbf{(3)}$$

- a kinetic equation for biomass growth:

$$\frac{dC_X}{dt} = R_X(C_S, C_X) \qquad \textbf{(4)}$$

where **u** = velocity vector, p = pressure, ρ = liquid density, ν = liquid kinematic viscosity, D = substrate diffusion coefficient, R_S and R_X = rates of substrate consumption and biomass formation respectively, and C_S and C_X = concentration of substrate and biomass respectively.

The order of magnitude of time constants for convective and molecular transport, biomass growth, biomass decay and detachment can be easily calculated. It can be shown that biomass growth and detachment rates are usually much slower than the rate of substrate diffusion into the biofilm. Hydrodynamics (momentum transport by convection or dissipation) is much faster than diffusive mass transfer. Therefore, while solving the mass balance equation, the flow can be considered at pseudo-equilibrium for a given biofilm shape, and at the same time the biomass growth, decay and detachment are frozen processes. This leads to the following strategy in following the biofilm development in time (Fig. 1):

1. First, a hydrodynamic step is performed. Momentum transfer (2) and continuity (1) equations are solved to find the flow field variables: pressure (p), velocities (**u**), the normal and tangential stresses (τ) acting on the biofilm surface. This step is needed each time the geometry of the system changes, for instance, by growth (a positive development) or detachment (negative development). The flow pattern will be considered completely established when the mass transfer calculations are executed.
2. The second step uses the just calculated flow velocities (**u**) in solving the convective - diffusive mass transfer of soluble components (substrates, products). Mass balance equation (3) is solved towards a pseudosteady-state concentration of substrate, C_S. The substrate concentration in turn will be used in the biomass growth kinetic equation. This is allowable because the time constant of bacterial growth is very slow compared to the diffusive substrate transfer. Both the first and second step of the model algorithm was performed using a lattice Boltzmann algorithm [3, 11]. In the absence of convection however, we preferred a finite-difference algorithm for solving the diffusion-reaction mass balance of substrate [9].
3. The new biomass content of each grid element, C_X, is calculated by using the Herbert-Pirt equation (4) including the substrate concentration at steady-state previously calculated.
4. As biomass increases it is redistributed in space according to discrete (cellular automata) rules as used by Picioreanu *et al.* [9.10] by splitting the biomass content in the elements in which a maximum biomass density was attained, and then by pushing the neighbours to reach the free space. This competition for space and for substrate generates the biofilm structure. On the other hand, this structure determines further development of the biofilm by changing the flow behaviour and nutrient transport.
5. A detachment step can also be performed before redistribution, because the detachment time constant falls in the same range as the growth time constant (10^5 s). Perhaps this is the reason why biofilm structure is determined by the balance between a positive process, growth, and negative processes such as detachment and decay. If positive and negative terms in this balance have very different values, the biofilm will either develop infinitely (growth is not balanced by detachment) or not develop at all (detachment dominates growth). By using a traditional finite-element method we can compute the deformation

energy in the biofilm induced by the fluid stresses at the biofilm surface. In this way we can determine where the biofilm will break. After the biofilm has lost some biomass, the external structure changes again and a new hydrodynamic step is necessary.

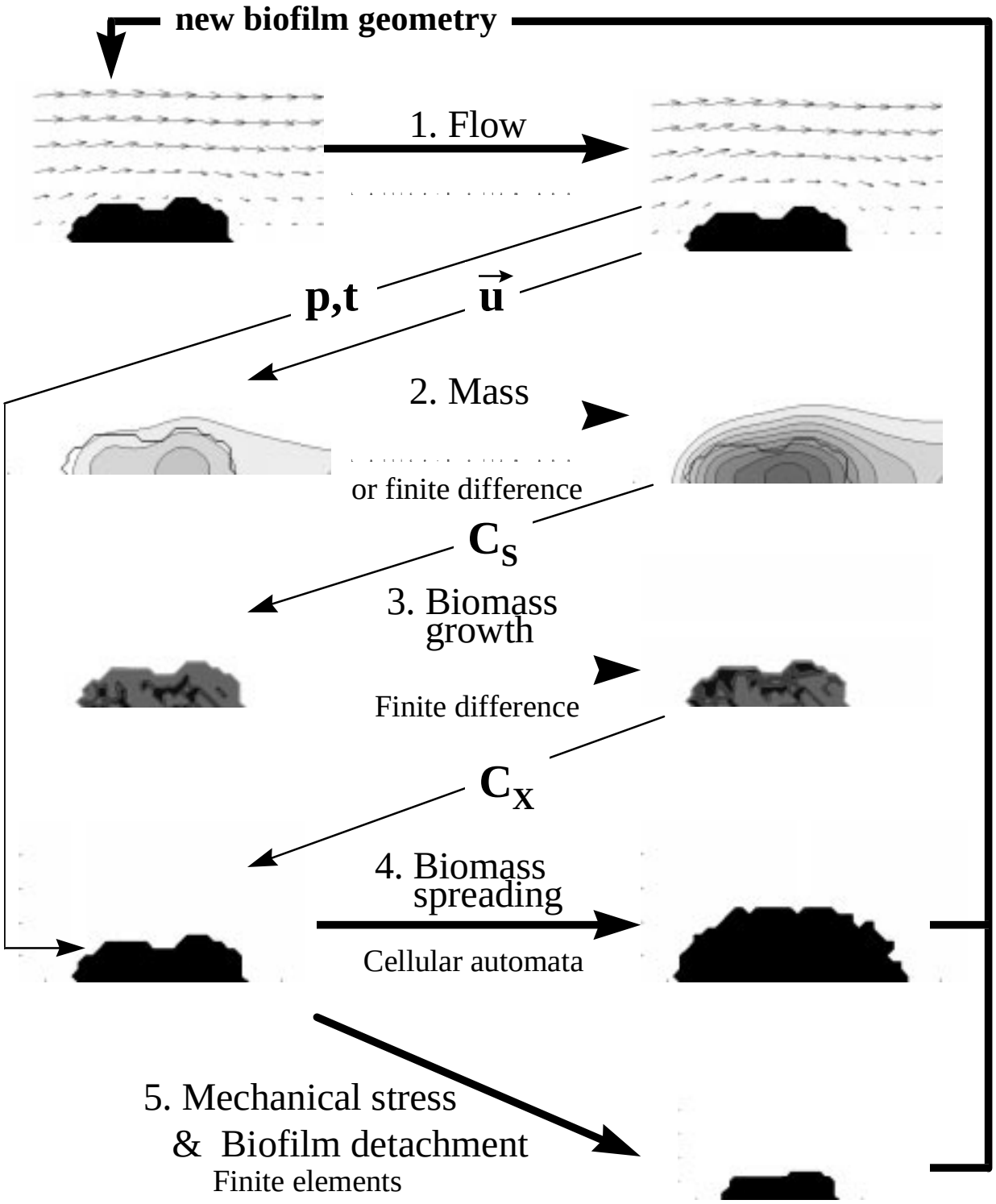

Figure 1. General algorithm used to solve the dynamic biofilm model

Model Applications

Results of the model as applied to a few particular cases are presented below. A simplified version of the model (DRG model), including only step 2, diffusional mass transfer of substrate, together with step 3, substrate conversion (Reaction) to biomass, and step 4, biomass Growth, runs both in a 2-D and 3-D space. The number of grid nodes is limited to $8 \cdot 10^6$ (a 200^3 cube). An extension of this model (CDRG model), which includes flow calculation around the biofilm structure (step 1), takes into account convective and diffusive substrate transfer, reaction, and biomass growth. This model is limited to 2-D calculations on maximum 10^6 grid nodes on a computer with 128 MB memory.

The development of a nitrifying biofilm under oxygen limiting conditions was studied. The biomass growth and substrate uptake kinetics used are presented in Picioreanu *et al.* [9, 10] and the model parameters are shown in Table 1.

Table 1. Parameters used in the biofilm model.

Model parameter	*Symbol*	*Parameter value*		*Units*
		DRG-3D	CDRG-2D	
Computational grid dimensions	$N_X \times N_Y \times N_Z$	100×100×80	200×200	-
Physical system dimensions	$L_X \times L_Y \times L_Z$	400×400×320	1000×1000	μm
Bulk oxygen concentration	C_{S0}	10^{-2} and $0.5 \cdot 10^{-3}$	$4 \cdot 10^{-3}$	kgS m^{-3}
Biomass maximum specific growth rate	μ_m	$1.5 \cdot 10^{-5}$	$1.5 \cdot 10^{-5}$	s^{-1}
Maintenance coefficient	m_S	$3 \cdot 10^{-5}$	$3 \cdot 10^{-5}$	kgS kgX^{-1} s^{-1}
Oxygen saturation constant	K_S	$0.35 \cdot 10^{-3}$	$0.35 \cdot 10^{-3}$	kgS m^{-3}
Biomass yield on substrate	Y_{XS}	0.045	0.045	kgX kgS^{-1}
Maximum biofilm biomass density	C_{Xm}	70	70 and 7	kgX m^{-3}
Oxygen diffusion coefficient	D	$1.6 \cdot 10^{-9}$	$2 \cdot 10^{-9}$	m^2 s^{-1}
Liquid kinematic viscosity	ν	-	10^{-6}	m^2 s^{-1}
Liquid density	ρ	-	1000	kg m^{-3}
Maximum liquid velocity in input	$u_{X,max}$	-	0.001, 0.004 and 0.01	m s^{-1}
Concentration boundary layer thickness	δ	$40 \cdot 10^{-6}$	calculated	m
Number of grid elements inoculated	n_0	1000 on plate 20 on sphere	5 and 15	-

Diffusion, Reaction and Growth Model

The DRG simplification of the general model assumes that the substrate coming from the bulk liquid diffuses through the CBL and biofilm matrix and is consumed by the bacteria and used for growth [10]. The concentration boundary layer is parallel to the carrier surface, has a constant thickness in time, and moves upwards as the biofilm thickness increases. Although these assumptions seem trivial, they can still be a realistic approximation for a system with a very slow liquid flow over the biofilm (see the oxygen microelectrode measurements by de Beer and Stoodley [1].

The results of such 3-D models [10] suggest that, in a mass transfer limited regime, the biofilm develops as a heterogeneous structure, presenting pores, channels and "mushroom"-like bacterial clusters (Fig. 2a), whereas in a substrate non-limited regime, a compact, and densely-packed biofilm forms (Fig. 2b). The non-quantitative models of Wimpenny and Colasanti [15] and Hermanowicz [5] show the same trend. Biofilm morphology can, however, be quantified by measures such as surface roughness (σ), surface area enlargement (A_f), fractal dimension of the surface (F), biofilm compactness (C_P) or porosity (ε), as defined in Picioreanu *et al.* [10]. By plotting these measures against the ratio between maximum biomass growth rate and maximum substrate transport rate (G), the effect of different growth regimes on biofilm structure can be clearly seen (Fig. 3).

One of the advantages of a discrete approach is that, once the model equations have been developed the boundary conditions and the geometry of the system can be easily changed. The carrier surface, for instance, can be spherical (Fig. 4) instead of flat. One can in this way model the development of biofilms in particle reactors (fluidized bed, airlift, etc.).

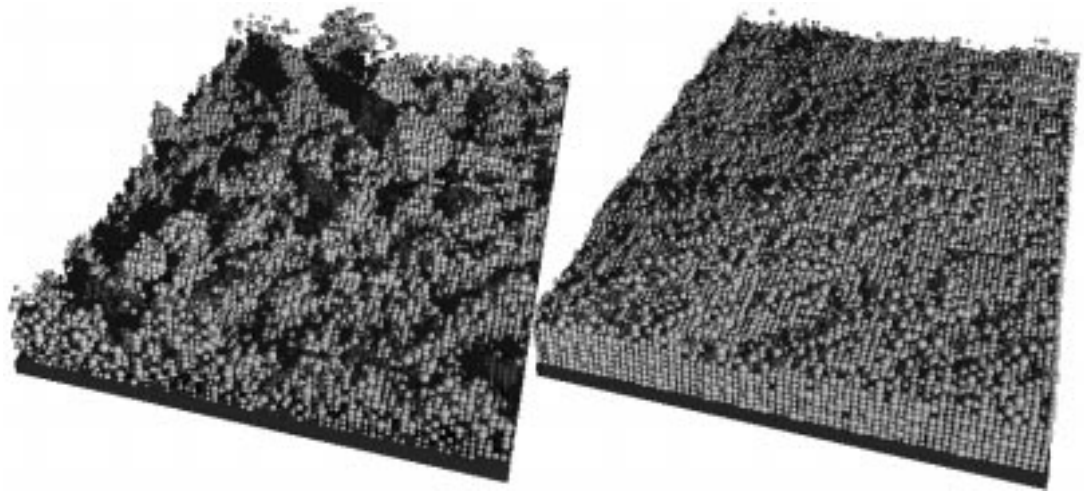

(a) (b)

Figure 2. Three-dimensional simulations of biofilm development on a planar surface in (a) substrate transfer limited regime after 10 days (b) biomass growth limited regime after 2 days. The biomass concentration at each grid node is proportional with the size of the particles used in this 3-D visualisation.

Convection, Diffusion, Reaction and Growth Model

The two-dimensional CGRG model was used to investigate the role of different environmental conditions on the biofilm evolution.

At high Reynolds numbers $Re = u_{X,\max} L_Y / \nu$, the external resistance to mass transfer diminishes by decreasing the thickness of both hydrodynamic and concentration boundary layers (Fig. 5a,b,c). This has an effect of smoothing the biofilm surface. Conversely, at lower *Re* (i.e., low fluid velocities) the thickness of CBL increases producing a rough biofilm. Pores and channels form in the biofilm as a result of nutrient depletion between the different bacterial colonies. Due to the steep gradient of substrate concentration, the biofilm top layer will grow much faster than the bottom layer giving a finger-like shaped biofilm.

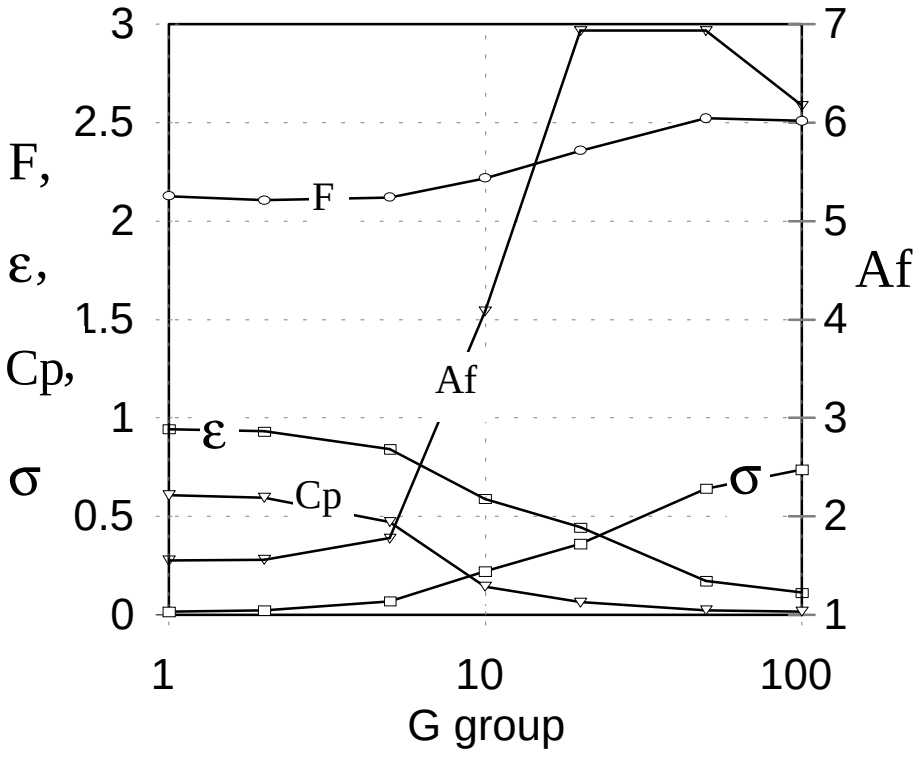

Figure 3. Influence of biomass growth rate/substrate transfer rate ratio (G group) on some biofilm characteristics.

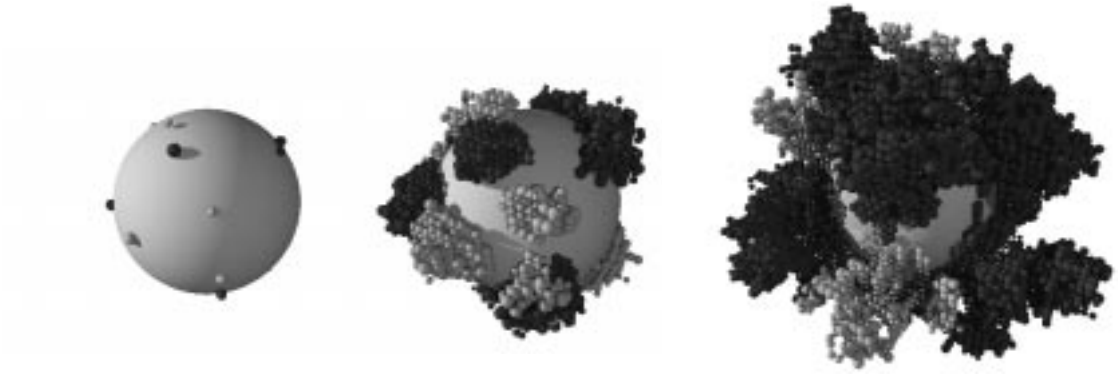

Figure 4. Simulated evolution in time of a two-species biofilm grown on a spherical carrier (mass transfer limited regime). The biomass concentration at each grid node is proportional with the size of the particles used in this 3-D visualisation. Two bacteria, with different growth characteristics, are shown as dark and light coloured balls.

The internal resistance to mass transfer, characterised by the Thiele number $\phi^2 = L_Y{}^2 C_{Xm}\left(\mu_m / Y_{XS} + m_S\right) / \left(D_S\, C_{S0}\right)$, influences biofilm formation in the same way. High ϕ^2 (given by a high specific substrate consumption rate, high biomass concentration C_{Xm}, low substrate diffusivity in the biofilm D, or low substrate concentration in the liquid C_{S0}) makes the biofilm structure more heterogeneous (Fig. 5a,b,c,d). At low ϕ^2 (high internal substrate transfer rate) the resulting structure is more compact and homogeneous (Fig. 5e,f) because the substrate penetrates deeper into the biofilm.

At a small number of initially attached cells (n_0), the resulting biofilm is made of large colonies separated by large, deep channels. When the carrier surface is densely populated at the initial stages, a rough biofilm with narrow channels will develop. In comparing the position of inoculum cells on the substratum with the actual spreading of the colony (Fig. 6), the bacterial colonies naturally extend in the direction of maximum substrate availability (to the left side and upward, in this case). There is therefore no need to introduce an *explicit* microscopic rule for a preferential direction of bacterial division.

The full 2-D model including detachment by erosion and sloughing is still being tested and its results will be presented in future. However, preliminary results show that an increasing detachment rate has two effects on the biofilm structure. First, the biofilm surface becomes smoother by continuous erosion forces that remove the small irregularities popping-up on the surface. Secondly, when the biofilm strength (E_a) decreases, the biofilm thickness and biofilm volume decrease as a result of both erosion and sloughing (Fig5c,g,h).

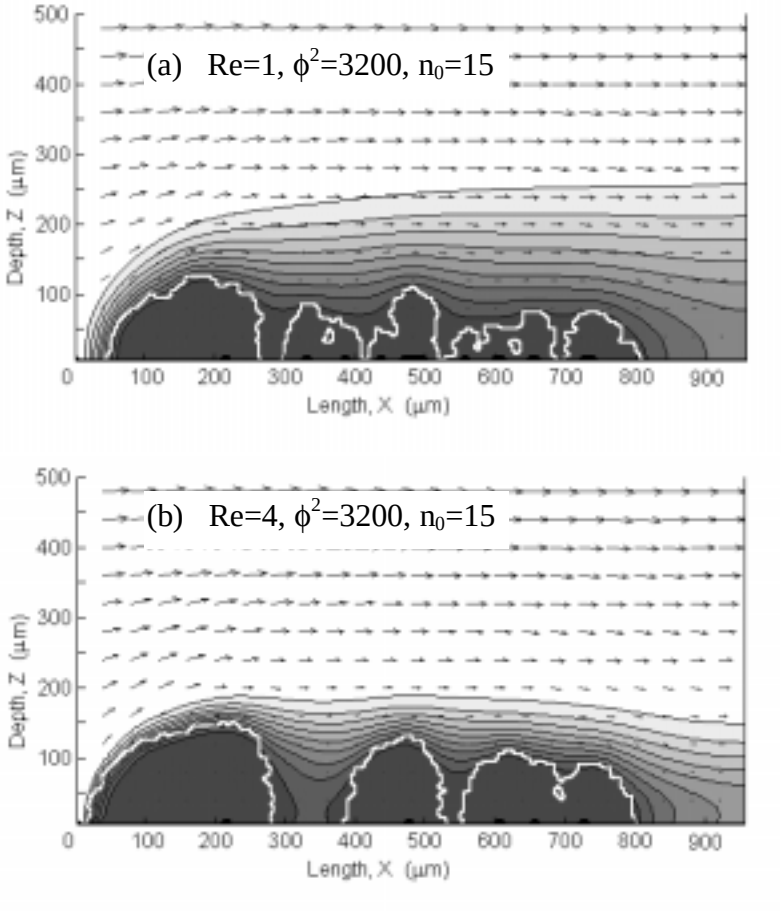

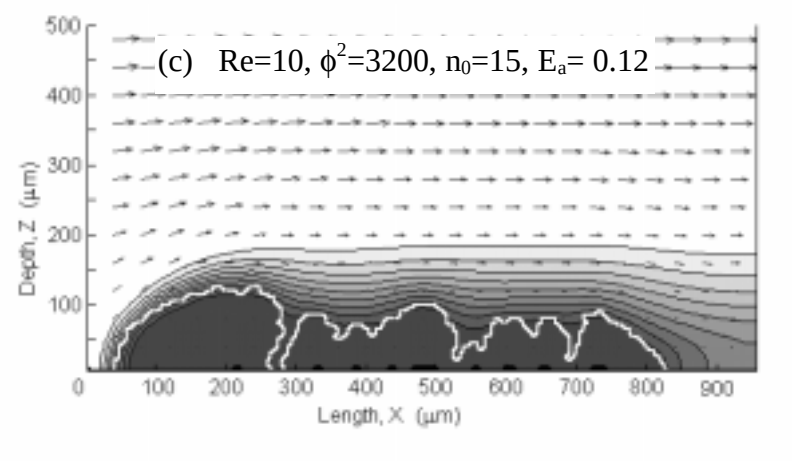
(c) Re=10, ϕ^2=3200, n_0=15, E_a= 0.12
Depth, Z (μm)
Length, X (μm)
0
100
200
300
400
500
600
700
800
900

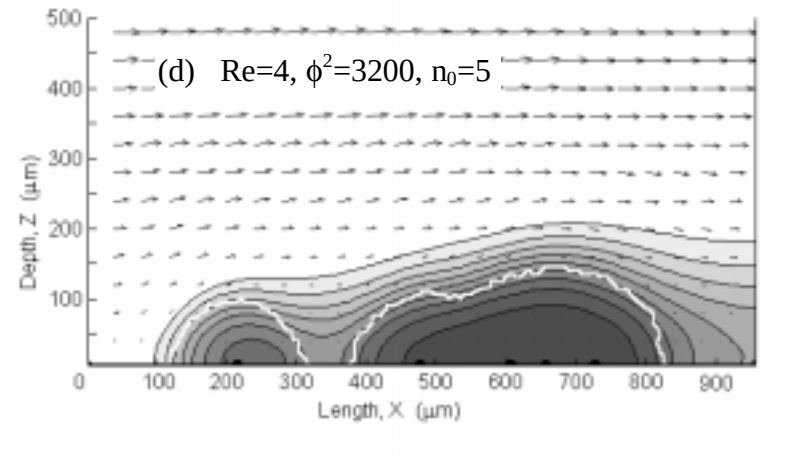
(d) Re=4, ϕ^2=3200, n_0=5
Depth, Z (μm)
Length, X (μm)
0
100
200
300
400
500
600
700
800
900

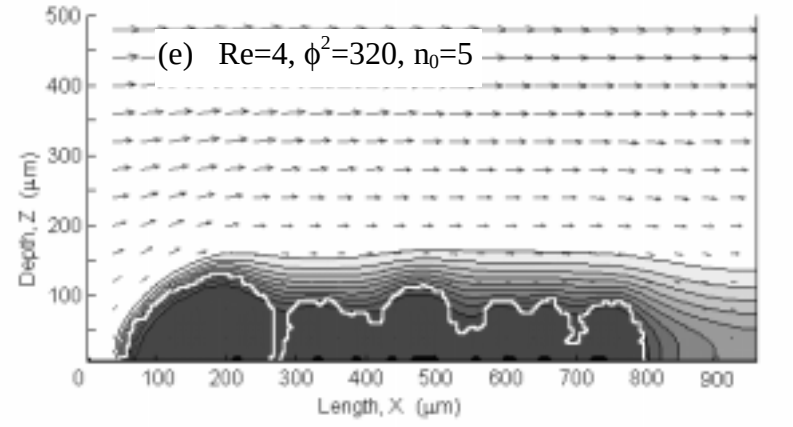
(e) Re=4, ϕ^2=320, n_0=5
Depth, Z (μm)
Length, X (μm)
0
100
200
300
400
500
600
700
800
900

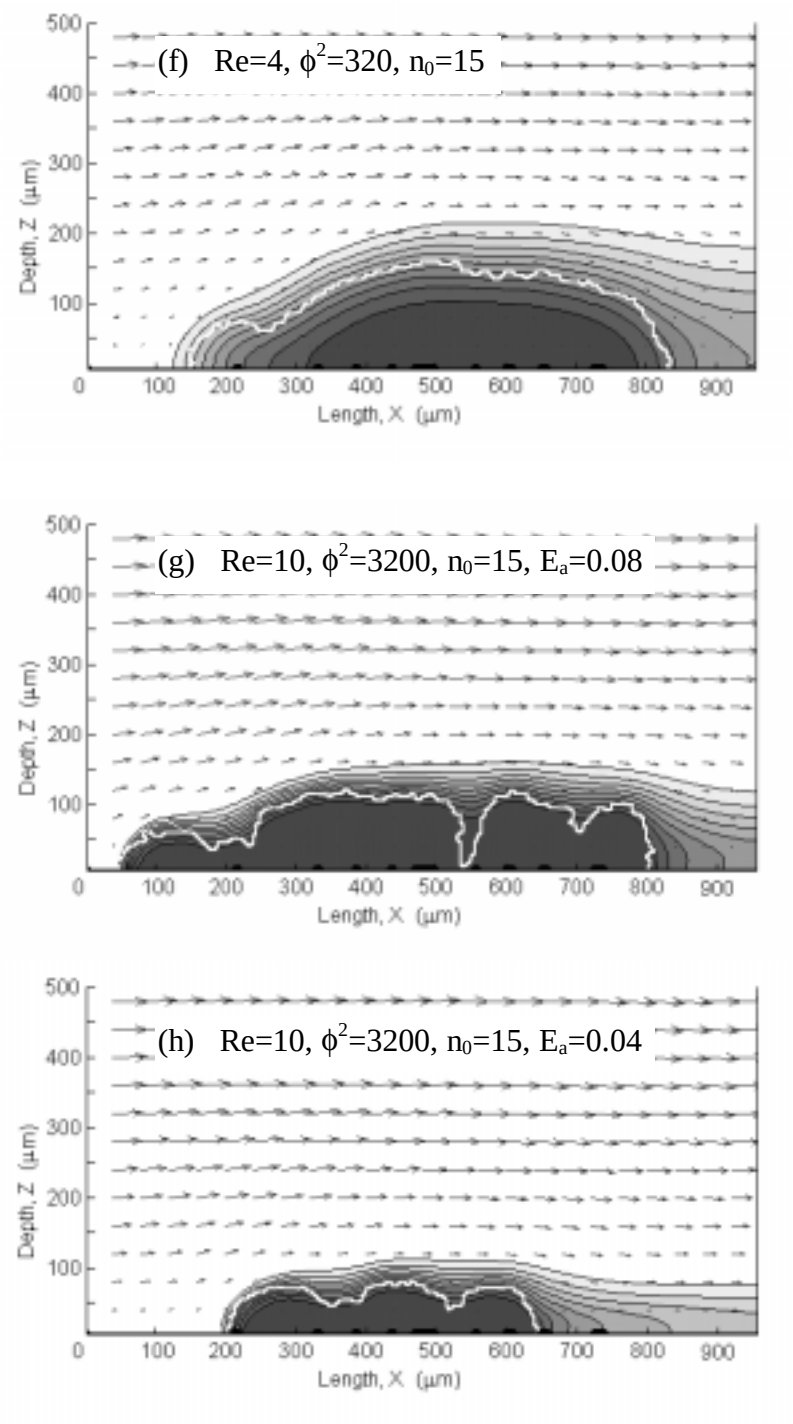

Figure 5. Two-dimensional simulations of biofilm development under flow conditions: biofilm state after (a) 14 days (b),(d) 10 days, (c), (g),(h) 9 days and (e),(f) 3 days. The biofilm surface is shown by a thick white line. The arrows represent the averaged value of vector velocity on a 8×8 square of grid nodes. Black lines indicate iso-concentration contours of substrate (10% increment between lines) from the maximum value in the bulk liquid (white region) to the areas depleted in substrate (dark grey regions). The black spots show the position of inoculum cells.

Conclusions

- A good, fully quantitative model approach has been developed. The multidimensional model includes biofilm processes such as fluid flow over irregular biofilm surface, substrate transport by convection and diffusion, substrate consumption and biomass growth. Incorporation of biofilm detachment is presently being studied. Moreover, commonly used physical, chemical and biological parameters (e.g., reaction rate constants, diffusivities, component concentrations and fluid velocities) can be directly used in the model.
- System geometry can be easily modified by changing the boundary conditions. The model can cope with any arbitrary substratum shape. It can also be easily adapted to represent multispecies and multisubstrate biofilm systems, making it a very useful tool for studying many aspects of biofilm ecology.
- Different biofilm structures, ranging from compact structures to porous and channelled structures, are generated by the model. The results support a previously postulated mechanism for biofilm structures [12]. A heterogeneous biofilm with rough surface and high porosity occurs in the slow substrate transfer regime, which is generated either by slow flow (high external mass transfer resistance) or by small substrate diffusivity in the biofilm (high internal resistance to mass transfer). In a non-limiting substrate case, generated by fast flow and fast internal diffusion, the biofilm develops as a compact structure.
- High shear forces lead, by means of continuous erosion, to a smoother, more compact and thinner biofilm. Discrete sloughing events, however, create a rougher biofilm.

Acknowledgements

This research is funded by the Netherlands Organisation for Applied Scientific Research (TNO) - contract 95/638/MEP.

References

1. de Beer D, Stoodley P (1995) Relation between the structure of an aerobic biofilm and transport phenomena. Wat Sci Tech 32:11-18
2. Bishop P, Rittmann BE (1996). Modelling heterogeneity in biofilms: Report of the discussion session. Wat Sci Tech 32:263-265
3. Chen S, Dawson SP, Doolen GD, Janecky DR, Lawniczak A. (1995). Lattice methods and their applications to reacting systems. Computers Chem Engng 19:617-646
4. Gjaltema A, Arts PAM, van Loosdrecht MCM, Kuenen JG, Heijnen JJ (1994). Heterogeneity of biofilms in rotating annular reactors: Occurrence, structure and consequences. Biotechnol Bioeng 44:194-204
5. Hermanowicz SW (1998). A model of two-dimensional biofilm morphology. Wat Sci Tech 37:219-222
6. Kugaprasatham S, Nagaoka H, Ohgaki S. (1992). Effect of turbulence on nitrifying biofilms at non-limiting substrate conditions. Wat Res 26:1629-1638
7. Kwok WK, Picioreanu C, Ong SL, van Loosdrecht MCM, Ng WJ, Heijnen JJ (1998). Influence of biomass production and detachment forces on biofilm structures in a biofilm airlift suspension reactor. Biotechnol Bioeng 58:400-407
8. Picioreanu C. (1996). Modelling biofilms with cellular automata. Final report to European Environmental Research Organisation, April 1996, Wageningen, The Netherlands.

9. Picioreanu C, van Loosdrecht MCM, Heijnen JJ (1998a). A new combined differential-discrete cellular automaton approach for biofilm modelling: Application for growth in gel beads. Biotechnol Bioeng 57:718-731
10. Picioreanu C, van Loosdrecht MCM, Heijnen JJ (1998b). Mathematical modelling of biofilm structure with a hybrid differential-discrete cellular automaton approach. Biotechnol Bioeng 58: 101-116
11. Ponce Dawson S, Chen S, Doolen GD (1993). Lattice Boltzmann computations for reaction-diffusion equations. J Chem Phys 98:1514-1523
12. Van Loosdrecht MCM, Eikelboom D, Gjaltema A, Mulder A, Tijhuis L, Heijnen JJ (1995). Biofilm structures. Wat Sci Tech 32:235-243
13. Wanner O, Gujer W (1986). Multispecies biofilm model. Biotechnol Bioeng 28:314-328
14. Wentland EJ, Stewart P, Ching-Tsan H, McFeters GA (1996). Spatial variations in growth rate within Klebsiella pneumoniae colonies and biofilm. Biotechnol Prog12:316-321
15. Wimpenny JWT, Colasanti R (1997). A unifying hypothesis for the structure of microbial biofilms based on cellular automaton models. FEMS Microb Ecol 22:1-16